

PSFC/JA-03-3

**Pressure Profile Control of Internal Transport Barrier Plasmas
In Alcator C-Mod**

J. H. BOY, Y. LIN, D. MOSSessian, S. M. WOLFE,

K. Zhurovich, M.J. Greenwald, I.H. Hutchinson,
M. Porkolab, J.A. Snipes

February 2003

Plasma Science and Fusion Center
Massachusetts Institute of Technology
Cambridge, MA 02139 USA

This work was supported by the U.S. Department of Energy, Cooperative Grant No. DE-FC02-99ER54512. Reproduction, translation, publication, use and disposal, in whole or in part, by or for the United States government is permitted.

Submitted for publication to *Nuclear Fusion*.

Pressure Profile Control of Internal Transport Barrier Plasmas in Alcator C-Mod

J. E. Rice, P. T. Bonoli, C. L. Fiore, W. D. Lee, E. S. Marmor, S. J. Wukitch,
R. S. Granetz, A. E. Hubbard, J. W. Hughes, J. H. Irby, Y. Lin, D. Mossessian,
S. M. Wolfe, K. Zhurovich, M. J. Greenwald, I. H. Hutchinson, M. Porkolab and J. A. Snipes
Plasma Science and Fusion Center, MIT, Cambridge, MA 02139-4307

Abstract

Internal transport barrier (ITB) plasmas with peak pressures of 0.25 MPa and pressure gradients as large as 2.5 MPa/m have been produced in Alcator C-Mod using off-axis ICRF heating. The onset of the ITBs is apparent when the pressure gradient exceeds 1.0 MPa/m, which is similar to the JET criterion of $\rho^*_s/L \geq 0.014$. Concomitant with the peaking of the core pressure as the ITB develops is a drop of the toroidal rotation velocity profile inside of the barrier foot; the maximum of the velocity gradient coincides with the peak in the pressure gradient. The quasi-coherent (QC) mode, associated with the enhanced D_α (EDA) H-mode plasmas which evolve the ITBs, breaks up and disappears as the barriers develop, even though the measured edge pedestal parameters remain fixed. The position of the ITB foot has been moved over a range of 1/3 of the plasma minor radius by varying the toroidal magnetic field. The peak in the calculated bootstrap current density profile has correspondingly been regulated over a similar range in plasma minor radius. The location of the density profile foot is found to expand as the toroidal magnetic field is reduced and the ICRF frequency is lowered. The density foot radius is relatively independent of q_{95} , however, in a scan of the plasma current at fixed B_T and wave frequency.

1. Introduction

The enhanced energy confinement and driven bootstrap current of plasmas with internal transport barriers (ITBs) render them an attractive choice for advanced tokamak operation. ITBs have been formed in normal and reversed magnetic shear configurations, by a variety of means (neutral beam injection, electron cyclotron heating, ion cyclotron range of frequencies (ICRF) heating, lower hybrid and electron cyclotron current drive, current ramping, pellet injection) in a large number of devices and have been observed in both the ion and electron channels. Recent comprehensive reviews of ITB plasmas may be found in Refs.[1,2]. Most ITBs are produced at relatively low densities ($\leq 10^{20}/\text{m}^3$), with decoupled electrons and ions, not necessarily in reactor relevant regimes with $T_e \sim T_i$. Most ITBs are also generated with substantial external momentum input from neutral beam injection, which may not be available in reactors. In exception to these cases are the ITBs observed in Alcator C-Mod [3-6], which are created at high densities with ICRF waves, and which appear in some Ohmically heated discharges. These ITBs are also distinct from those observed in other devices in that the barrier is most evident in the electron density profile, with no strong ion temperature peaking; this may be a consequence of high electron-ion coupling. Since it is the pressure gradient that leads to the attractive attributes of enhanced energy confinement and bootstrap current, and because the density and temperature gradients contribute equally, it is important to consider these ITBs in the context of more conventional barriers formed by neutral beam injection, with strongly peaked temperature profiles.

While there is no universally accepted definition of an ITB, and as such no generally agreed upon criterion for their formation, much progress has been made in both the theoretical understanding and in the experimental production of these plasmas [7,8,1,2]. Formation of ITBs can occur when the $\mathbf{E} \times \mathbf{B}$ shearing rate exceeds the maximum growth rate for drift wave driven microturbulence, whence the thermal conductivity and particle diffusivity drop, resulting in improved energy and particle confinement [9-11]. Gradients in velocity and/or pressure (temperature

and/or density) can contribute to this shearing rate, which can stabilize turbulence driven by ion and electron temperature gradient (ITG and ETG) and trapped electron (TEM) modes. Magnetic shear and the Shafranov shift can also help to lower the turbulence growth rates.

In order to take advantage of the beneficial features of ITB plasmas, it is desirable to demonstrate control of barrier parameters and performance. For reactor applications, it is imperative to maintain ITB plasmas in steady state, and barriers formed with transient current ramping do not lead to steady state. Furthermore, to increase the volume of the good confinement region, the ITB region must be expanded radially outward [12,13]. For tailoring of the bootstrap current density profile, it is necessary to adjust the ITB foot location, which has been achieved through external current drive schemes [12]. Finally, it is obligatory to demonstrate the control of impurities within the barrier region, which tend to accumulate in accordance with the improved particle confinement. Steady state density and impurity control has been achieved in Alcator C-Mod [5,6] and ASDEX Upgrade [14] plasmas using on-axis ICRF heating.

A brief description of ICRF experiments on Alcator C-Mod is given in the next section. In Section 3 pressure and pressure gradient profile evolution in ITB discharges are presented and a comparison with the JET criterion [15] for ITB formation is given. Impurity toroidal rotation velocity profiles and some observations of the QC mode relevant to ITB evolution are also shown. Movement of the ITB foot location and control of the inferred bootstrap current density profile are demonstrated in Section 4, followed by conclusions.

2. Experimental Setup

The Alcator C-Mod [16] tokamak is a compact device (major radius $R = 0.67$ m, typical minor radius of 0.21 m), which can operate with strong shaping ($\delta_U \leq 0.85$, $\delta_L \leq 0.80$, $\kappa \leq 1.8$), usually in the lower single null configuration. For the

experiments described here, the on-axis toroidal magnetic field was in the range $3.7 \leq B_T \leq 6.5$ T and plasma currents were between 0.5 and 1.2 MA. Up to 4 MW of ICRF power at 80 MHz are available, and the power is coupled to the plasma by 2 two-strap antennas, each with $0 - \pi$ phasing; the cases described here are with H minority heating in deuterium plasmas. On-axis heating occurs for this frequency at a toroidal magnetic field of 5.3 T. ITBs have been produced with off-axis ICRF heating on the high magnetic field side (HFS) with $B_T < 4.5$ T [3,4], and on the low magnetic field side (LFS) with $B_T > 6.1$ T. An additional 4 MW of ICRF power are available from a variable frequency (40-80 MHz), variable phase four-strap antenna; for the cases described here, this antenna was operated with $0 - \pi - 0 - \pi$ phasing at a frequency of 70 MHz, which provides on-axis heating for $B_T = 4.6$ T. ITBs have also been produced with off-axis ICRF heating at 70 MHz both on the HFS with $B_T < 3.9$ T and on the LFS with $B_T > 5.2$ T [5]. Central electron densities in these ITB plasmas have been obtained in the range from $3 \times 10^{20}/\text{m}^3$ to nearly $1 \times 10^{21}/\text{m}^3$. ITBs have also been obtained using pellet injection, in purely Ohmic plasmas and at H- to L-mode back transitions which occur in most discharges [4]; these cases will not be discussed here.

Electron density profiles were determined by Thomson scattering and from the visible continuum using a high spatial resolution imaging CCD system [17]. Comparison of these *Bremsstrahlung* profiles with the electron density profiles measured by Thomson scattering, which has only six spatial locations in the core plasma, allows $Z_{\text{eff}}(r)$ to be determined. The Z_{eff} profiles were interpolated, and used to convert the *Bremsstrahlung* profiles into full electron density profiles with fine spatial resolution. This correction is proportional to $\sqrt{Z_{\text{eff}}}$ and is typically less than 20%. Electron temperature profiles were determined from Thomson scattering and from electron cyclotron emission (ECE).

Previous measurements of toroidal rotation velocities [3,5] in Alcator C-Mod ITB plasmas have been largely restricted to the magnetic axis ($r/a=0$). There are now two additional vertically displaced tangentially viewing high resolution x-ray

spectrometers which provide impurity toroidal rotation velocities at $r/a = 0.3$ and $r/a = 0.6$.

3. ITB Formation

The formation of ITBs in Alcator C-Mod is identified by a distinct peaking of the electron density profile which occurs in conjunction with a large drop in the core toroidal rotation velocity [3,5]. Parameter time histories for a typical ITB discharge are shown in Fig.1. This 4.5 T, 770 kA plasma entered H-mode at 0.678 s after application of 2 MW of 80 MHz ICRF power (the resonance location was near $r/a = 0.5$ on the HFS), as evidenced by the increases in the plasma stored energy, central electron density, central electron and ion temperatures and core toroidal rotation velocity. Just before 0.9 s, the velocity began to drop (and eventually reverse direction) and the central electron density began to increase, indicating the ITB formation. Density profiles with a peaking factor ($n_e(0)/n_e(r/a=0.7)$) over 4 and a central value of nearly $1 \times 10^{21}/\text{m}^3$ have been achieved transiently in similar discharges. These profiles, which evolve in the absence of an external particle source, have been modeled with a low core particle diffusivity ($\sim .01 \text{ m}^2/\text{s}$), and an inward convection equal in magnitude to the Ware pinch velocity [6]. The ion temperature profiles however do not show such a dramatic central peaking, or a distinct break in slope usually characteristic of ITB plasmas [5]. This may be because at high electron densities with tightly coupled electrons and ions, the electron thermal conductivity is dominating the heat transport. Even though the density was steadily increasing during the ITB formation in Fig.1, and although the ICRF heating was directed well off-axis, at $r/a \sim 0.5$, the core electron and ion temperatures rose and remained steady until 1.1 s, indicating a drop of the central thermal conductivity between 0.7 and 1.1 s. This has been confirmed with TRANSP modeling [18,5] and through heat pulse propagation analysis [6], which conclude that the core χ drops to $\sim 0.1 \text{ m}^2/\text{s}$ during the ITB phase. There is no universally accepted definition of an ITB,

but a factor of 10 reduction in the *core* particle and thermal transport coefficients certainly is well described by the name ‘internal transport barrier’.

A criterion for the presence of ITBs has been developed for JET plasmas [15], having a form that is convenient to evaluate experimentally and is based on theoretical principles: an ITB exists when the ratio of the ion Larmor radius at the sound speed (ρ_s is a characteristic length which appears in the dispersion relations for ITG modes and TEMs) to the local temperature gradient scale length exceeds a critical value, or $\rho^*_T \equiv \rho_s / L_T = c_s / \omega_{ci} / L_T \geq 0.014$. A similar value has been found for FTU ITB plasmas [19]. For JET plasmas, the electron temperature scale length, L_{T_e} , was chosen for the evaluation because high spatial and temporal resolution electron temperature profiles are routinely and readily available. It could be argued that the local pressure gradient scale length, $L_P = -P(\partial P / \partial r)^{-1}$, is also relevant, both theoretically [11] and experimentally, for the formation and identification of ITBs, since the $\mathbf{E} \times \mathbf{B}$ flow is proportional to the pressure gradient. For Alcator C-Mod ITB plasmas, it is the electron density profile which is available with high spatial and temporal resolution [17], and which allows for high resolution pressure profiles. (For high density, low field ITBs on C-Mod, the ECE is usually cut off.) Shown in Fig.2 is the time evolution of the pressure profile ($2 \times n_e(r) \times T_e(r)$, since full ion density and temperature profiles were unavailable) for the discharge of Fig.1. For the fully developed ITB, the central value of the pressure was 0.25 MPa. The flex point of the profiles as the barrier evolved was at $r/a \sim 0.4$. In Fig.3 are shown the pressure gradient profiles for the discharge of Fig.2. The ITB was initially apparent in the bump at $r/a=0.35$, which exceeded 1 MPa/m for the profile at 0.9 s (green dotted line). In other similar discharges, the first evidence for ITB formation is seen in modifications to sawtooth heat pulse propagation [6]. For the fully developed ITB at 1.2 s, the maximum pressure gradient was nearly 2.5 MPa/m. Finally, plots of $\rho^*_P \equiv \rho_s / L_P$ profiles for this discharge are shown in Fig.4, along with the JET criterion number of 0.014, which is in good agreement with the Alcator C-Mod profiles. Perhaps a value of 0.012 would be a better match (lower limit value), based on the rotation and density profile information at 0.9 s. (The feature near $r/a=0.6$

in Fig.4 is an artifact.) This suggests that the JET criterion is more uniformly applicable with use of the pressure gradient scale length, and furthermore, that the underlying ITB formation mechanism(s) may be similar for a wide variety of plasma conditions, production techniques and operational regimes. According to a temperature profile stiffness definition [1,20], however, these C-Mod barriers are not ITBs since there is no distinct change in the temperature gradients.

The previous discussion concerned the criterion for distinguishing the existence of an ITB, but did not address the underlying mechanism(s) for ITB formation. One candidate process is the suppression of turbulence via strong shear in the plasma rotation [10]. Clearly toroidal rotation is involved in the ITB development process in Alcator C-mod plasmas [3,5], as shown in Fig.1, even though the rotation generating mechanism is unknown [3]. In the previous measurements, little could be said about the rotation shear since the off-axis spectrometer views had only a small toroidal angle. A total of three separate tangential views is now available, covering $r/a = 0, 0.3$ and 0.6 . The time histories of the toroidal rotation velocity from these three views for the discharge of Fig.2 are shown in Fig.5. Immediately following the H-mode transition, the velocity increased at the edge of the plasma and propagated inward on a time scale similar to the energy confinement time. The evolution of the toroidal velocity profile between 0.67 and 0.80 s is consistent with pure momentum diffusion from an (unknown) edge source, and a momentum confinement time of ~ 150 ms, about a factor of four larger than the energy confinement time. The velocity reached a maximum of ~ 35 km/s (co-current) by 0.8 s, with a relatively flat profile (see Fig.6). The ITB began to form around 0.87 s, at which time the velocity profile inside of the ITB foot ($r/a < 0.5$) collapsed (reduced from a substantial co-current speed to near zero) in about 200 ms. Outside of the ITB foot ($r/a = 0.6$), the velocity decreased on a longer time scale, and didn't reduce to zero or reverse direction. The toroidal rotation profile evolution for this discharge is shown in Fig.6. During Ohmic L-mode, the profile was flat and slightly counter-current [21]. After entering H-mode, the plasma began to rotate in the co-current direction, in the absence of external momentum input [22,23]. In fact this co-current rotation

propagated in from the outside, as the profile changed from hollow at 0.7 s to flat at 0.85 s, in accordance with momentum diffusion of an edge source. After the barrier formation, the rapid collapse of the core rotation inside of the ITB foot ($r/a \sim 0.47$) is evident in the profile at 1.0 s. Unfortunately the adjacent rotation views on either side of the ITB foot are separated by a third of the minor radius, or about 7 cm, so only a lower limit to the toroidal velocity gradient of $3 \times 10^5 \text{ s}^{-1}$ can be given in the vicinity of the foot; this velocity gradient could easily be a factor of three or more higher. The rotation velocity gradient is greatest where the pressure gradient is largest. This estimate of the shearing rate [11] may be compared with calculated [24,25] growth rates ($\sim 10^6/\text{s}$) for ITG turbulence. The time evolution of the radial electric field profile can be estimated from this crude toroidal rotation velocity profile using the calculated neo-classical [26] impurity rotation [3]. E_r determined in this fashion is demonstrated in Fig.7. The electric field was positive in the core of the plasma during the normal EDA H-mode phase, then reversed direction in the core as the ITB evolved. During the ITB phase, E_r varied in sign (from negative to positive) moving outward in the vicinity of the ITB foot, suggesting a negative E_r well. A lower limit to the electric field gradient of 250 kV/m^2 was determined near the maximum of the pressure gradient; this could be a factor of ~ 3 higher. While neither the cause for the co-current toroidal rotation in the initial H-mode phase nor that of the subsequent reversal in the core as the barrier develops is understood, the observed velocity gradient and inferred electric field gradient are consistent with the workings of velocity shear stabilization of ITG driven turbulence as the ITB evolves.

Other clues to the ITB formation mechanism(s) in Alcator C-Mod may be related to the various thresholds which have been observed. For ITBs spawned by off-axis ICRF heating, there is a sharp threshold in the resonance location for ITB production; the ICRF resonance must be outside of $|r/a|=0.5$. This was revealed by scanning the toroidal magnetic field for both HFS and LFS absorption at two separate frequencies, 70 and 80 MHz [3,5]. Interestingly, but not surprisingly, there is no such magnetic field effect for ITBs in purely Ohmic plasmas.

Another threshold for ITB generation via off-axis ICRF heating is in the density of the *target* plasma; for ITBs formed with HFS heating at 80 MHz and 4.5 T, the average electron density of the target plasma must be above $1.4 \times 10^{20} / \text{m}^3$ [5]. Plasmas whose L-mode target density is below this value do not develop ITBs, but remain in H-mode, in spite of the fact that after making the transition to H-mode, the density is then above this threshold! This density threshold is very close to the threshold that separates ELM-free from EDA H-mode [27]. ELM-free H-mode discharges (both Ohmic and ICRF) do not evolve into ITB plasmas; most ITB plasmas originate in EDA H-mode. One unique feature of EDA plasmas [28] is the presence of the ‘quasi-coherent’ (QC) mode [29-31], an oscillation with a frequency around 100 kHz, which has been observed with a variety of diagnostics: micro-wave reflectometry [32], phase-contrast-imaging (PCI) [31] and edge magnetic probes [30]. Ironically, once the ITB begins to form in the EDA H-mode plasma, its EDA character partly disappears. This is demonstrated in Fig.8, which shows the time evolution of the frequency spectrum of fluctuations measured with the 88 GHz reflectometer channel for the discharge of Fig.1. Just after the plasma entered EDA H-mode, the QC mode appeared, and settled in frequency to about 85 KHz, in this case. As the toroidal rotation velocity dropped and the ITB formed after 0.9 s, the QC mode broke up, as the frequency slightly increased. Similar behavior has been seen with the PCI and magnetic diagnostics, so this cannot simply be a feature of the edge electron density profile changing. In fact the edge electron density profile, determined from visible *Bremsstrahlung* and the edge Thomson scattering system, remained unchanged from 0.8 to 1.2 s during this discharge. Neither did the edge pedestal electron temperature profile, also measured by Thomson scattering, change shape during this time interval, although the magnitude of the temperature slowly dropped as the core density increased. The edge collisionality, however, did not change. It may be that the edge electric field evolved; it is known [31] that E has a profound influence on the QC mode.

4. Control of the ITB Foot Location

Control of the electron and impurity densities in ITB plasmas has been demonstrated using two frequency heating: off-axis heating to create the barrier, followed by on-axis heating to control the density [5,6]. It is also desirable to control the location of the ITB foot, to increase the volume of the high confinement region, or to drive the bootstrap current at a particular location. In ITBs produced in reversed magnetic shear configurations on other devices, the barrier foot is often located at the q minimum [33,34]; the foot can be moved by changing the current density profile either by ramping the current, or with external current drive [12]. In Alcator C-Mod, the q profiles are monotonic, with $q_{min} \sim r=0$, and the foot location is usually in the vicinity of the $q=3/2$ surface, not at $q=1$ which is near $r/a = 0.15$, based on the sawtooth inversion radius. The ITB foot has been moved over a range of a third of the minor radius with off-axis ICRF heating by varying the toroidal magnetic field. Shown in Fig.9 are electron density profiles from four different ITB discharges; at four magnetic fields corresponding to HFS and LFS absorption at both 70 and 80 MHz. The ITB foot locations are shown by the vertical lines. The widest ITB, with the foot located at $R=0.817$ m ($r/a \sim 0.6$), was obtained at 3.9 T with 70 MHz, HFS heating; the narrowest foot, at 0.758 m ($r/a \sim 0.3$), was with 80 MHz, LFS heating at 6.3 T. For this narrow ITB at 6.3 T, the drop in the central toroidal rotation during the ITB phase was only a factor of two, down to 20 km/s (co-current), and the QC mode did not break up completely. This trend of the outward movement of the foot at lower magnetic field suggests that operation at 60 MHz and 3 T would produce an ITB close to the EDA edge pedestal. The electron density foot location (as demonstrated in Fig.9) for a large number of discharges with nearly identical plasma current (in the range from 765 to 800 kA) for these four conditions (70 and 80 MHz, HFS and LFS) are shown in Fig.10 as a function of magnetic field. There is a steady decrease of the ITB size as the magnetic field is raised; the straight line is a linear fit to the measured points. This demonstrates the separation of the ICRF deposition location and the ITB foot. In all of these cases the resonance location was near $R = 0.792$ m ($r/a \sim 0.5$) based

on TORIC [35] calculations. The nominal values of q_{95} are shown in parentheses for each group of points. One possible conjecture is that as q_{95} is lowered, the ITB foot location expands. This hypothesis has been tested by scanning the plasma current for a series of otherwise similar discharges with HFS heating at 80 MHz and 4.5 T. The results for the location of the electron density ITB foot as a function of q_{95} are shown in Fig.11 by the red dots. (In some discharges there is a slight movement of the density foot location as the ITB evolves; these points represent the nominal positions averaged over the ITB period.) This corresponds to a range of plasma currents from 1.14 MA ($q_{95}=2.97$) to 565 kA ($q_{95}=6.01$). The density foot location was relatively insensitive to q_{95} during this plasma current scan, as all of these points were near $R = 0.79$ or $r/a \sim 0.47$. It should be noted that for some of these discharges, the electron density ITB foot was not in the same location as the χ_{min} determined from heat pulse propagation analysis. Also shown in the figure are the measured sawtooth inversion radii (purple triangles) and the positions of the $q=3/2$ surface as calculated from EFIT [36] (green + signs), which each vary in the expected fashion. The ITB density foot location does not obviously correlate with the $q=3/2$ surface position or the sawtooth inversion radius ($q=1$). Fig.10 suggests that the ITB foot location is a function of the magnitude of the toroidal magnetic field, and not strongly dependent on the plasma current or q_{95} . Since the shearing rate $\omega_{E \times B} \propto 1/B_T$ [9], it is easier at low magnetic field to exceed γ_{lin} , the linear growth rate for microturbulence, over a larger volume of the plasma, which allows the ITB foot to move outward. Also, in the JET criterion for ITB production, $\rho^*_P \propto 1/B_T$, so it is easier to exceed that limit at lower magnetic field.

One application for control of the ITB foot location is the regulation of the bootstrap current density profile; the range of this control is demonstrated in Fig.12 where the calculated bootstrap current density profiles for the widest and narrowest ITBs from Fig.9 are shown. For the 3.9 T, 70 MHz discharge, the bootstrap current was peaked near $r/a \sim 0.5$ while for the 6.3 T, 80 MHz discharge, the bootstrap current was peaked near $r/a \sim 0.2$.

5. Conclusions

ITB plasmas with peak pressures of 0.25 MPa and maximum pressure gradients of 2.5 MPa/m have been obtained in Alcator C-Mod. The presence of ITBs, when the ratio of ρ_s to the gradient scale length exceeds a threshold value, is found to be very close to the JET criterion of 0.014, if the pressure gradient is used. Other criteria for ITB formation with off-axis ICRF heating in Alcator C-Mod plasmas are that the resonance location be outside of $r/a \sim 0.5$ (for both HFS and LFS absorption) and that the average electron density of the target plasma be above $1.4 \times 10^{20}/\text{m}^3$. The plasma usually first enters EDA H-mode before it evolves an ITB. Formation of ITBs is accompanied by a substantial drop in the toroidal rotation velocity inside of the ITB foot. Outside of the foot the velocity reduction is not so strong, and a lower limit to the velocity gradient of $3 \times 10^5/\text{s}$ was observed in the vicinity of the maximum pressure gradient. E_r was found to be negative inside of the ITB foot and positive outside. Another observation for the EDA H-mode plasmas which form ITBs is that the QC mode breaks up as the core electron density peaks and the rotation velocity drops.

The ITB foot location has been expanded by lowering the toroidal magnetic field and ICRF frequency; the ITB density foot location decreases with increasing B_T , but is independent of q_{95} . This observation is consistent with $\omega_{\text{ExB}} \propto 1/B_T$. Control of the bootstrap current density profile has been demonstrated; the peak of the bootstrap current has been moved from $r/a \sim 0.2$ to 0.5.

6. Acknowledgements

The authors thank J. Terry for D_α measurements, S. Scott, M. Redi and D. Ernst for useful discussions, G. Schilling for assistance with the ICRF experiment and the Alcator C-Mod operations and RF groups for expert running of the tokamak and the ICRF systems. Work supported at MIT by DoE Contract No. DE-FC02-99ER54512.

References

- [1] R. C. Wolf, Plasma Phys. Control. Fusion **45** (2003) R1.
- [2] J. W. Connor et al., submitted to Nuclear Fusion (2003).
- [3] J. E. Rice et al., Nucl. Fusion **41** (2001) 277.
- [4] C. L. Fiore et al., Phys. Plasmas **8** (2001) 2023.
- [5] J. E. Rice et al., Nucl. Fusion **42** (2002) 510.
- [6] S. J. Wukitch et al., Phys. Plasmas **9** (2002) 2149.
- [7] E. J. Synakowski, Plasma Phys. Control. Fusion **40** (1998) 581.
- [8] C. Gormezano, Plasma Phys. Control. Fusion **41** (1999) B367.
- [9] T. S. Hahm and K. H. Burrell, Phys. Plasmas **2** (1995) 1648.
- [10] R. E. Waltz et al., Phys. Plasmas **2** (1995) 2408.
- [11] K. Burrell, Phys. Plasmas **4** (1997) 1499.
- [12] Y. Koide et al., Phys. Plasmas **4** (1997) 1623.
- [13] C. Gormezano et al., Phys. Rev. Lett. **80** (1998) 5544.
- [14] J. Stober et al., in Fusion Energy (*Proc. 19th Int. Conf., Lyon, 2002*), IAEA, Vienna, CD-ROM, IAEA-CN-94 EX/C3-7Rb
- [15] G. Tresset et al., Nucl. Fusion **42** (2002) 520.
- [16] I. H. Hutchinson et al., Phys. Plasmas **1** (1994) 1511.
- [17] E. S. Marmor et al., Rev. Sci. Instrum. **72** (2000) 940.
- [18] P. T. Bonoli et al., ‘Analysis of ICRF Heated Transport Barrier Experiments in Alcator C-Mod’ in *Proceedings of the 14th Topical Conference on Radio-Frequency Power in Plasmas, AIP Vol.595*, Oxnard, CA 2001, American Institute of Physics, Melville, New York (2001) p.178
- [19] V. Pericoli Rindolfini et al., in Fusion Energy (*Proc. 19th Int. Conf., Lyon, 2002*), IAEA, Vienna, CD-ROM, IAEA-CN-94 EX/C3-6
- [20] A. G. Peeters, et al., Nucl. Fusion **42** (2002) 1376.
- [21] J. E. Rice, et al., Nucl. Fusion **37** (1997) 421.
- [22] J. E. Rice, et al., Nucl. Fusion **38** (1998) 75.
- [23] J. E. Rice et al., Nucl. Fusion **39** (1999) 1175.

- [24] M. H. Redi et al., 29th European Physical Society Conference on Plasma Physics and Controlled Fusion, Montreux, Switzerland, 2002, P-1 .082
- [25] D. R. Ernst, et al., Bulletin of the American Physical Society Vol. 47 (AIP, NY, 2003) p. 139.
- [26] Y. B. Kim, P. H. Diamond and R. J. Groebner, Phys. Fluids B **3** (1991) 2050.
- [27] A.E. Hubbard, R.L. Boivin, R.S. Granetz *et al.*, Phys. Plasmas **8**, 2033 (2001).
- [28] M. Greenwald et al., Nucl. Fusion **37** (1997) 793.
- [29] M. Greenwald et al., Phys. Plasmas **6** (1999) 1943.
- [30] J. A. Snipes et al., Plasma Phys. Control. Fusion **43** (2001) L23.
- [31] A. Mazurenko et al., Phys. Rev. Lett. **89** (2002) 225004.
- [32] Y. Lin et al., Rev. Sci. Instrum. **70** (1999) 1078.
- [33] E. J. Strait et al., Phys. Rev. Lett **75** (1995) 4421.
- [34] T. Fujita et al., Phys. Rev. Lett. **78** (1997) 2377.
- [35] M. Brambilla, Nucl. Fusion **38** (1998) 1805.
- [36] L. L. Lao et al., Nucl. Fusion **25** (1985) 1611.

Figure Captions

Fig. 1 Time histories of (from top to bottom) the plasma stored energy, central electron density, central electron and ion temperatures, ICRF heating power and central toroidal rotation velocity, for a 4.5 T, 770 kA plasma. The dotted vertical line indicates the time of the L- to H-mode transition.

Fig. 2 Measured pressure profiles for the discharge of Fig.1. The profile during L-mode at 0.6 s is shown in purple. The profiles from the fully developed H-mode period at 0.8 s (solid green) through the fully formed ITB phase at 1.2 s (solid red) are from every 100 ms (green dotted:0.9 s, brown dashed:1.0 s, pink chain: 1.1 s).

Fig. 3 The magnitude of the pressure gradient profiles for Fig.2, with the same legend.

Fig. 4 $\rho^*_{P \equiv \rho_s} / L_P$ profiles for the discharge of Fig.2, with the same legend. The JET ITB criterion value of 0.014 is shown by the horizontal dotted line.

Fig. 5 Toroidal rotation velocity time histories for $r/a=0$ (red), $r/a=0.3$ (green) and $r/a=0.6$ (purple). The vertical dotted lines indicate the times of the H-mode transition (0.671 s) and the earliest appearance of the ITB (0.87 s).

Fig. 6 The evolution of the toroidal rotation velocity profiles from the time histories of Fig.5. In purple is the L-mode profile (.55 s), in green are the profiles during the H-mode formation (0.70 s) and pre-ITB EDA H-mode phase (0.85 s), and in red are the ITB profiles.

Fig. 7 E_r profiles from Fig.6. The green asterisks represent the radial electric field during the H-mode phase at 0.82 s, while the red dots are from the ITB phase at 1.1 s.

Fig. 8 The time evolution of the frequency spectrum of fluctuations observed on the 88 GHz reflectometer channel is shown in the top frame and the rotation velocity is shown in the bottom frame, for the discharge of Fig.1. During the normal H-mode phase, up until 0.85 s, the QC mode can be seen with a frequency near 85 kHz.

Fig. 9 Electron density profiles for four ITB discharges. Solid green: 3.9 T, HFS 70 MHz; solid red: 4.5 T, HFS 80 MHz; dashed green: 5.5 T, LFS 70 MHz; dashed red: 6.3 T, LFS 80 MHz. The vertical lines indicate the ITB foot locations.

Fig. 10 The ITB density foot locations as a function of toroidal magnetic field for discharges with plasma currents in the range from 765 to 800 kA. For each group of points, the nominal values of q_{95} are given in parentheses. 70 MHz: green asterisks; 80 MHz: red dots. The solid line is a linear fit.

Fig. 11 The ITB density foot locations as a function of q_{95} for discharges at 4.5 T with 80 MHz ICRF heating are shown as red dots. This corresponds to a range of plasma currents from 1.14 MA to 565 kA. The green + signs represent the calculated locations of the $q=3/2$ surfaces from EFIT, while the purple triangles are the measured sawtooth inversion radii from two x-ray arrays.

Fig. 12 The calculated bootstrap current density profiles for the 3.9 T (solid green) and 6.3 T (dashed red) discharges of Fig.9.

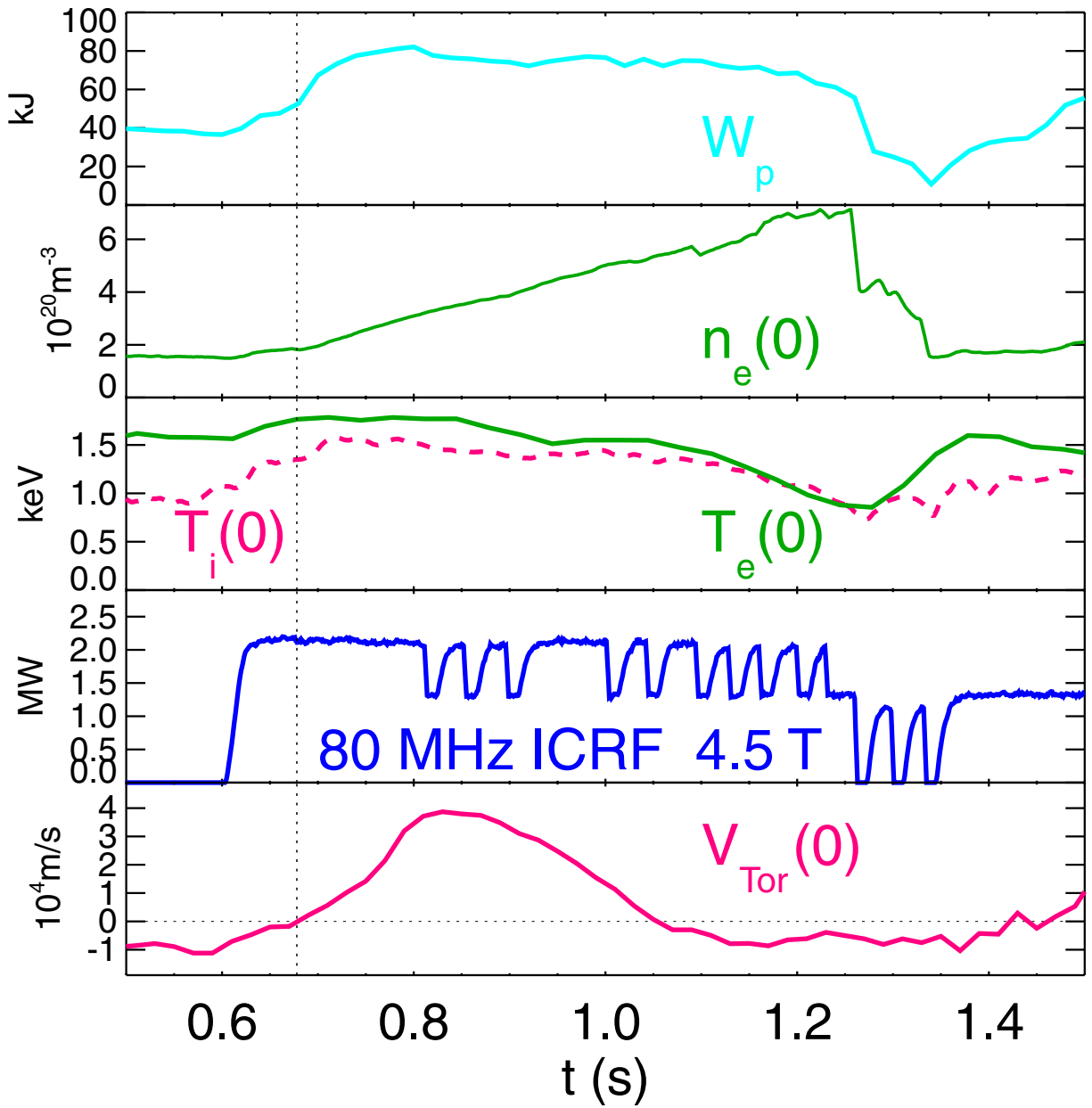
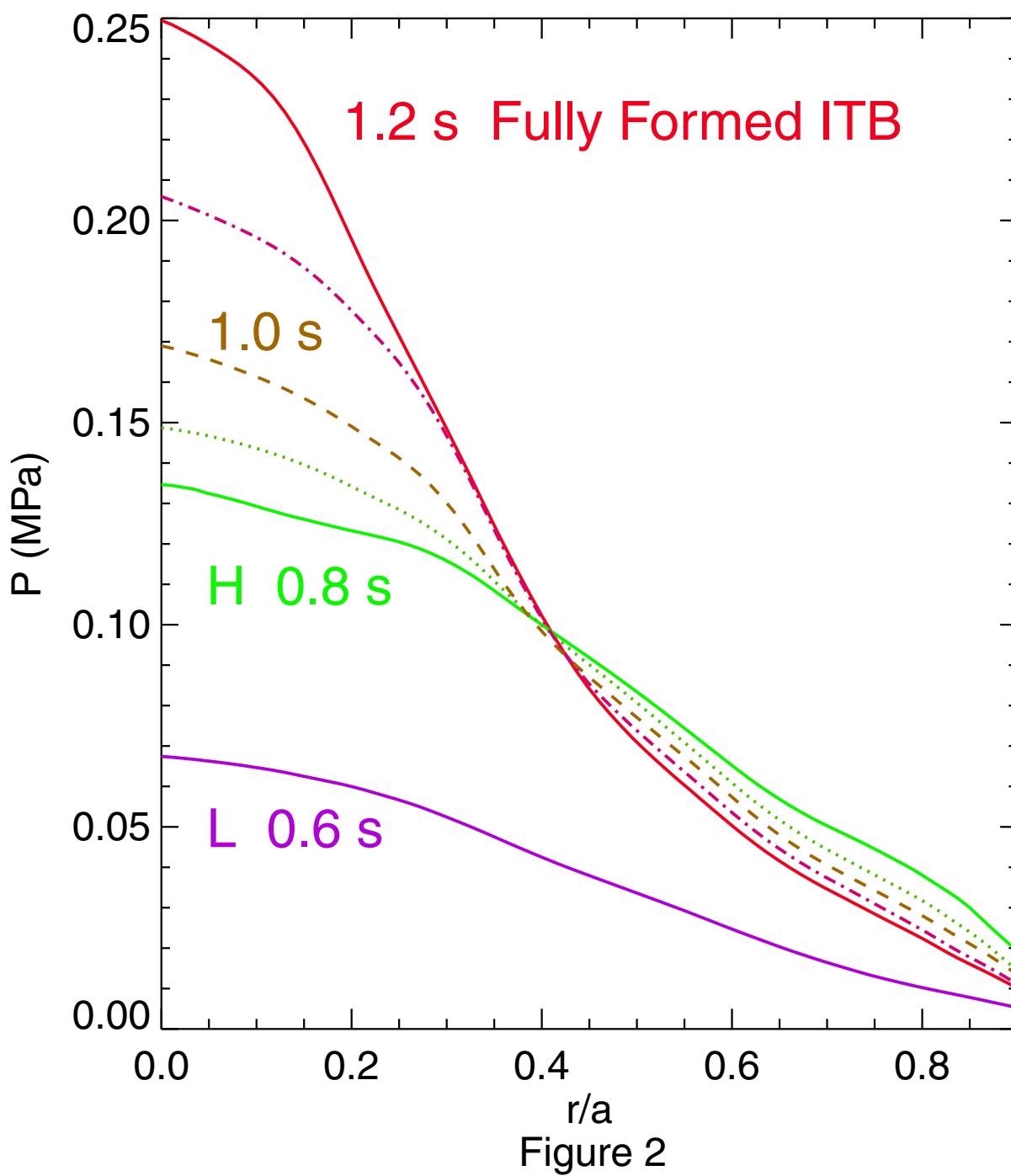


Figure 1



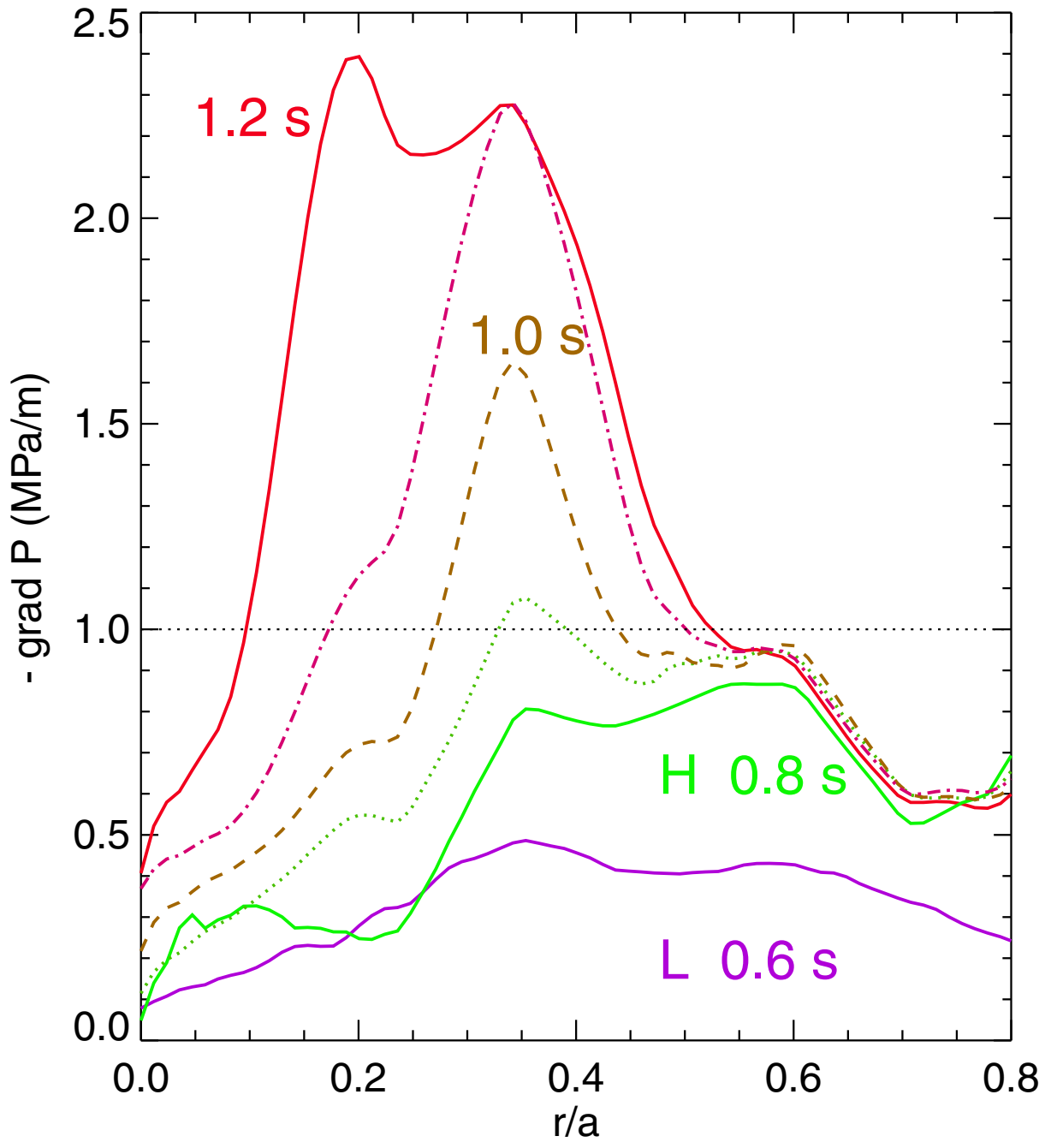


Figure 3

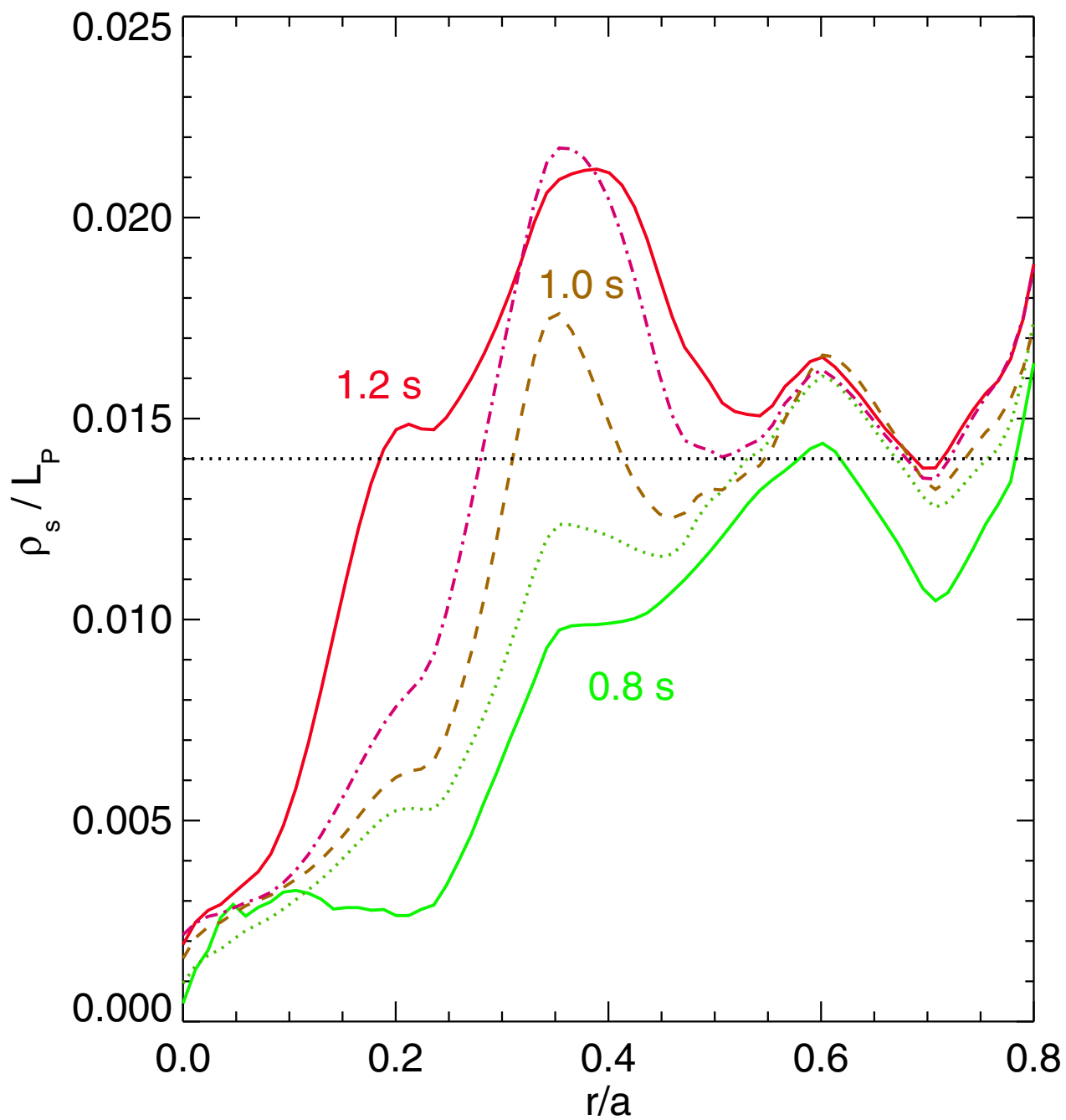


Figure 4

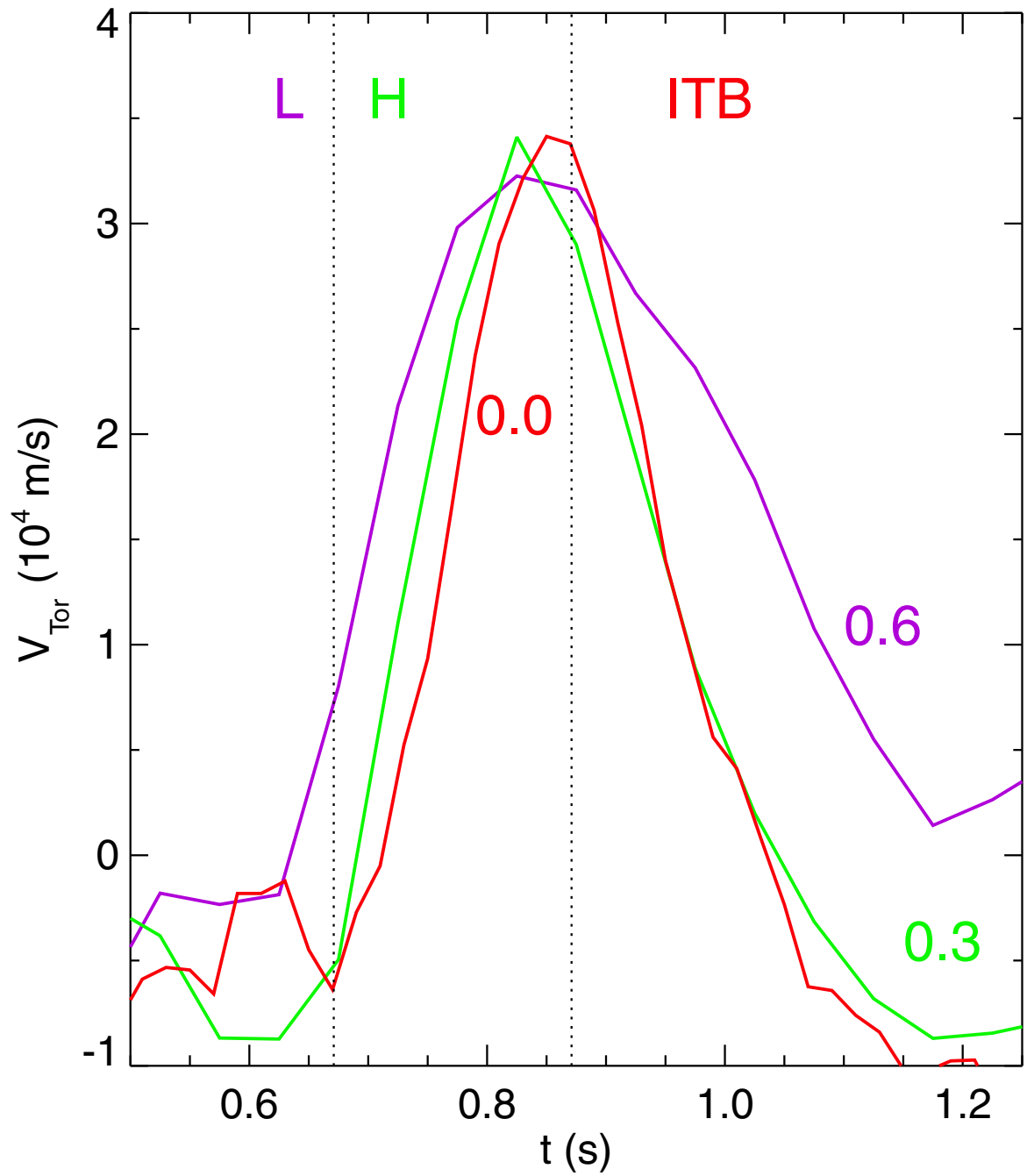


Figure 5

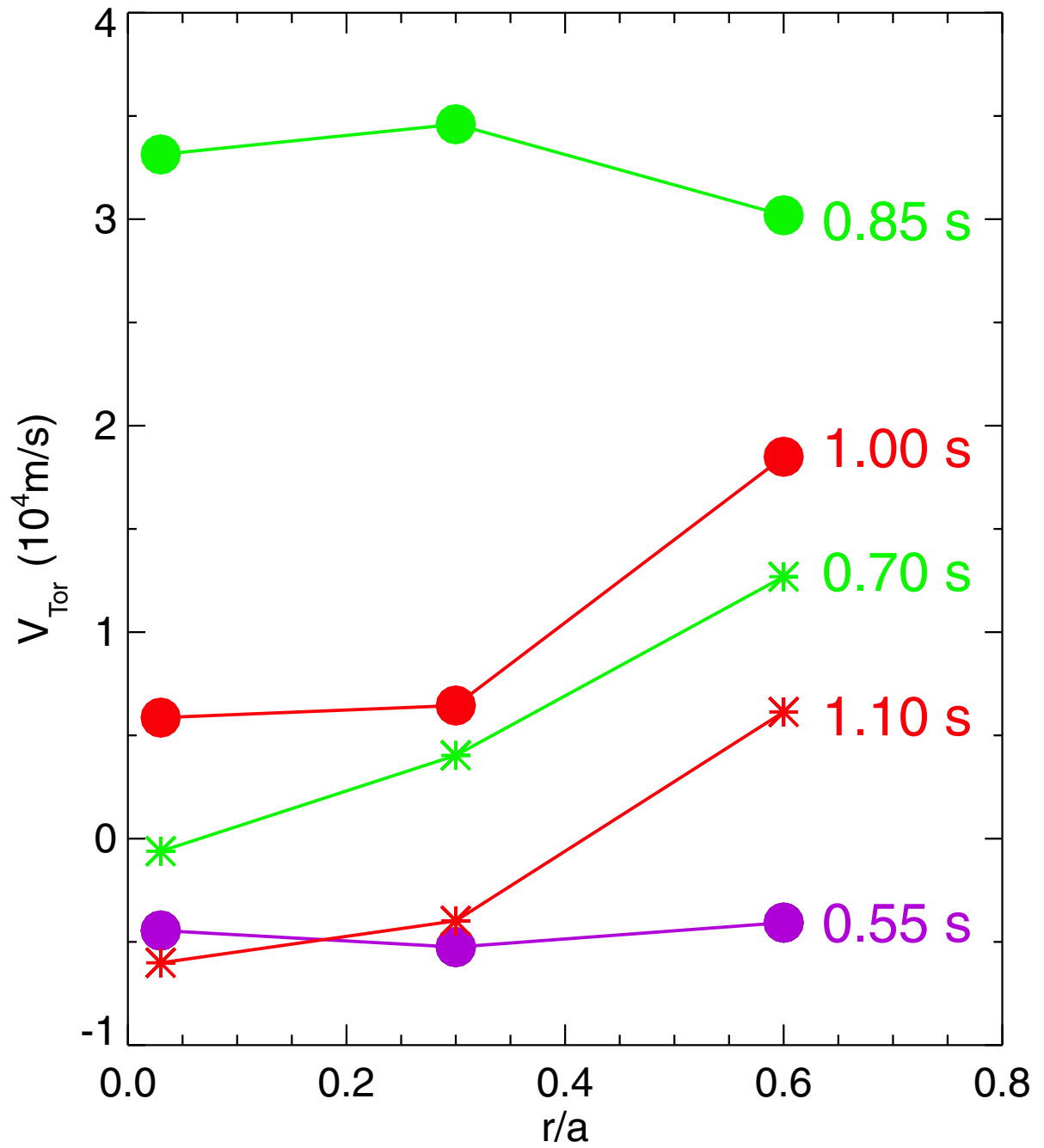


Figure 6

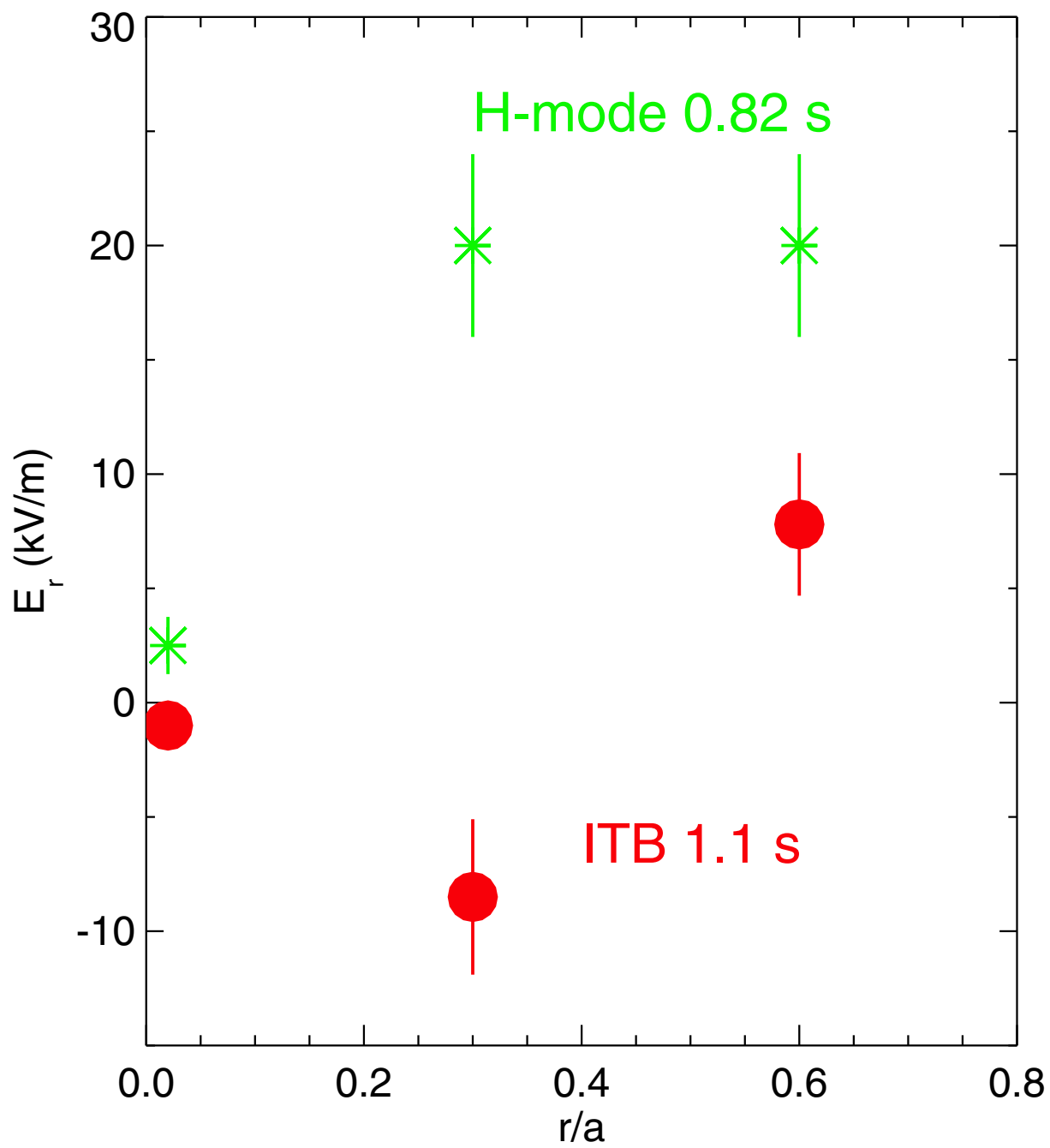


Figure 7

Shot 1020925007

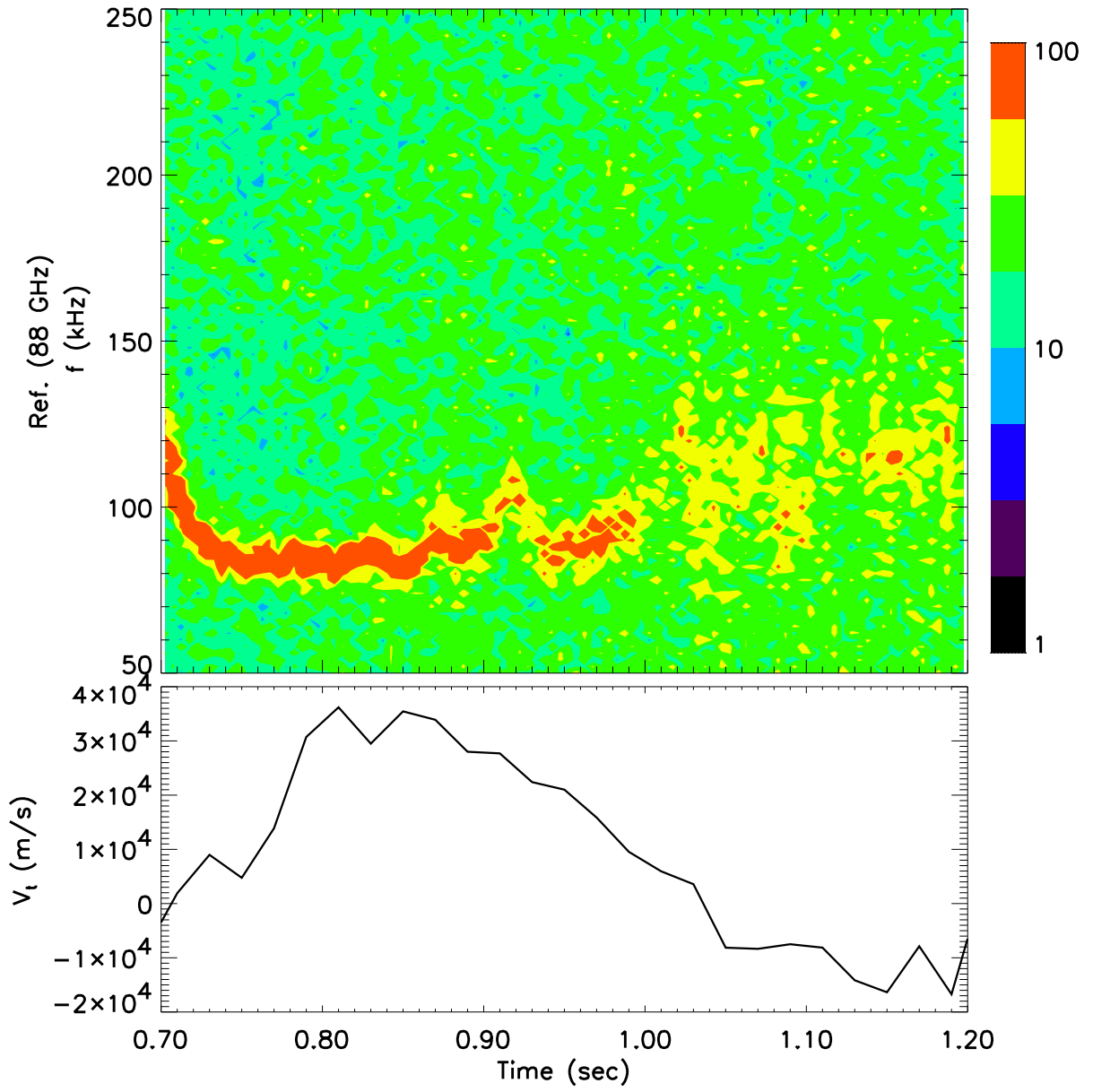


Figure 8

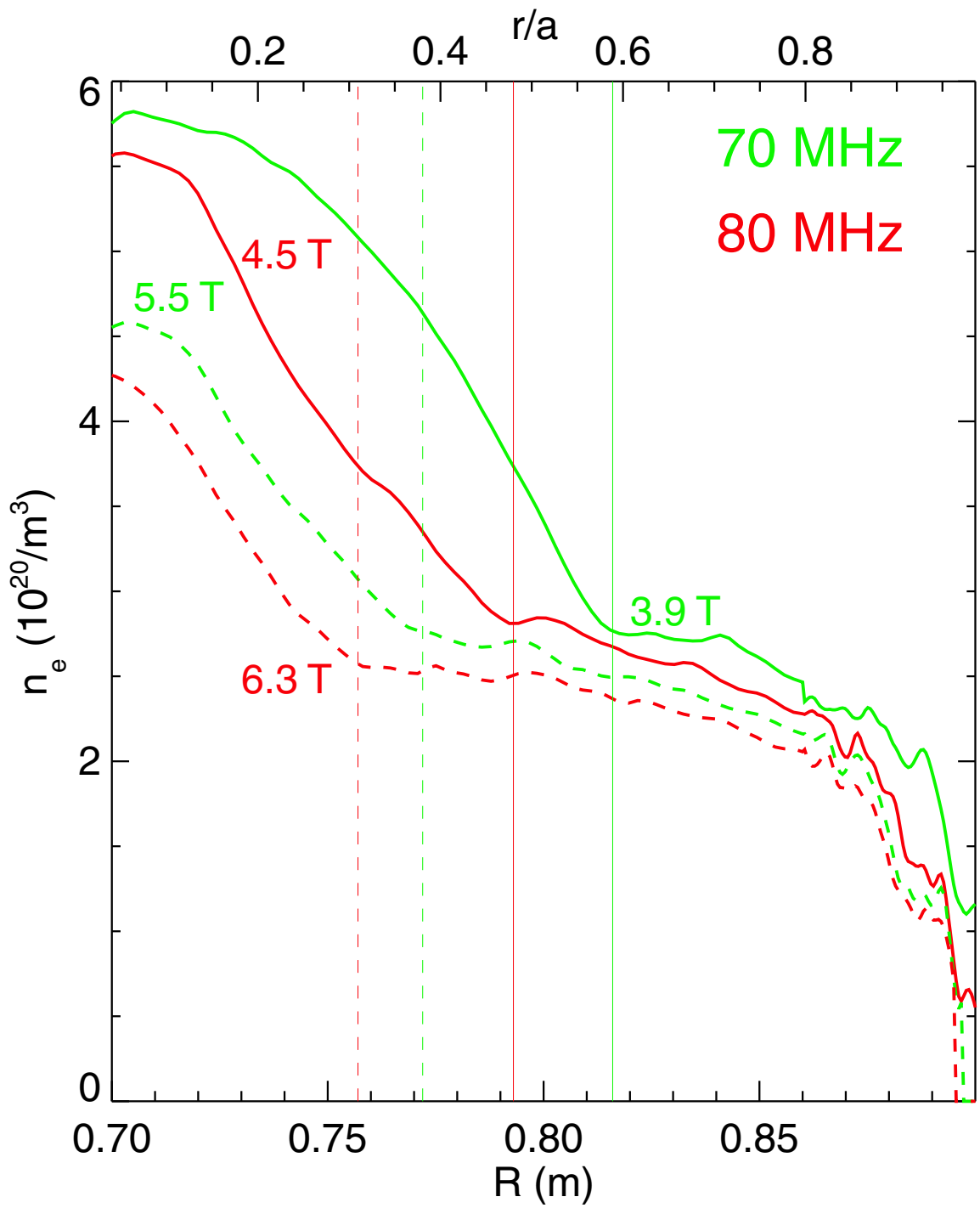


Figure 9

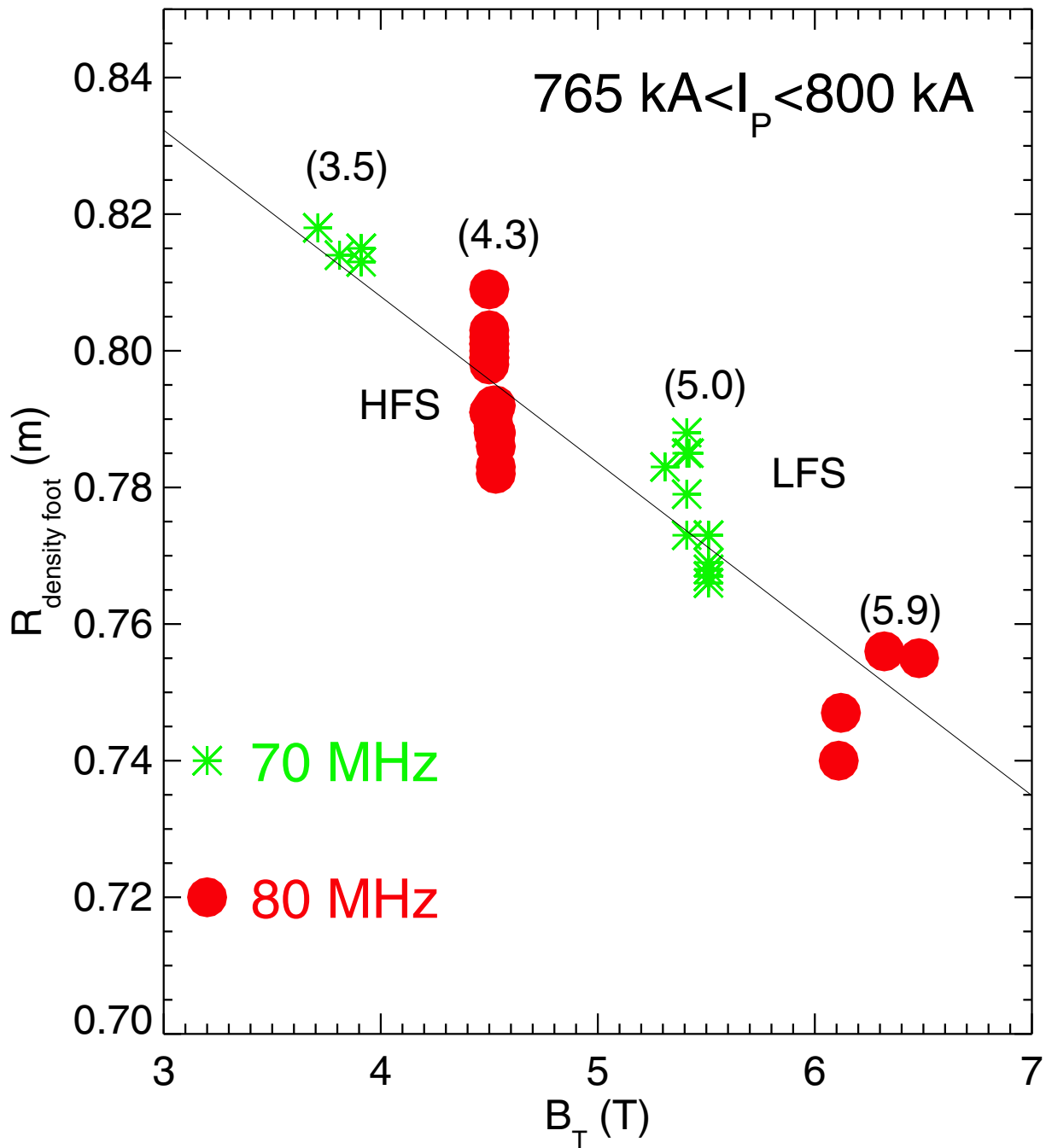
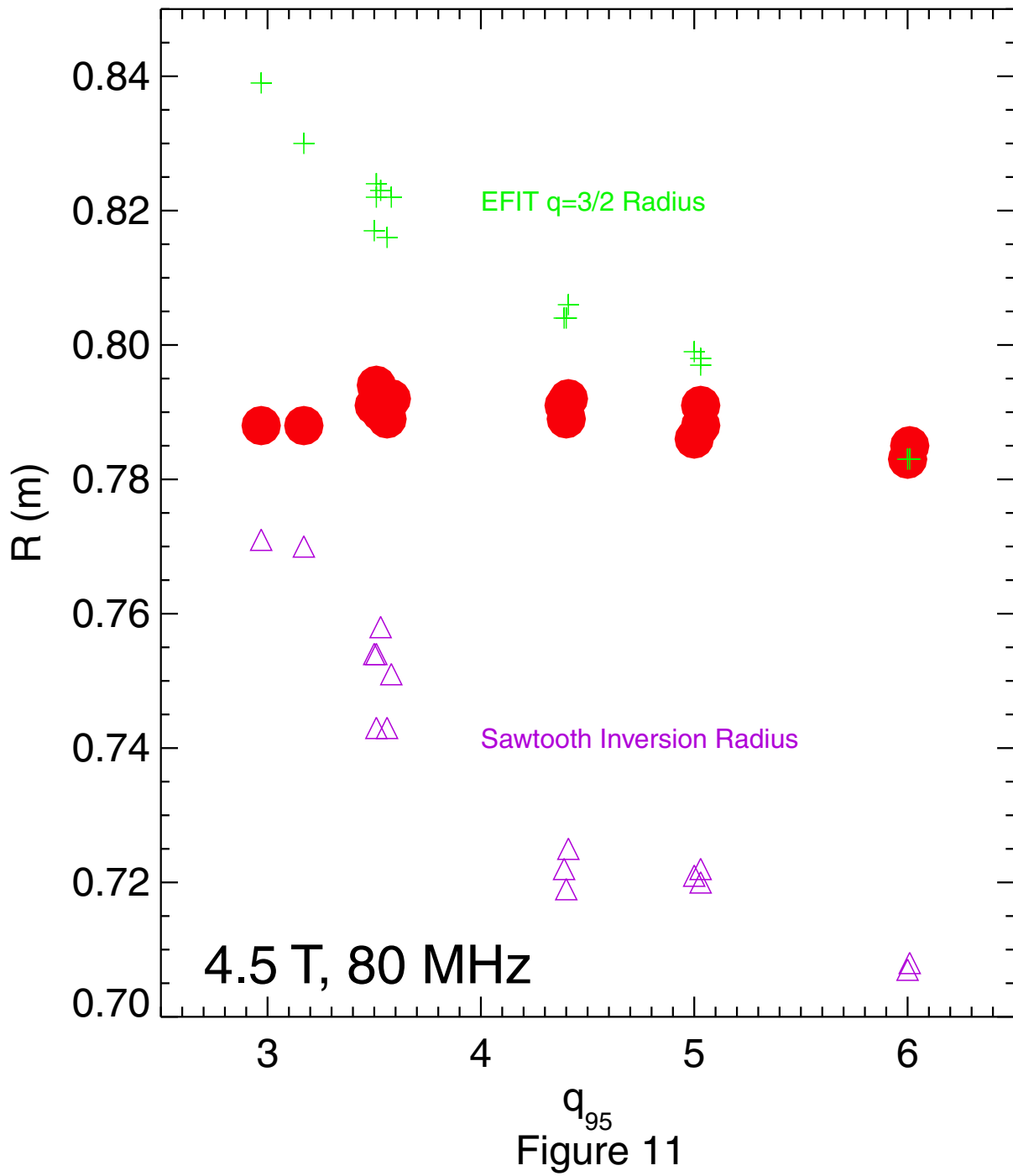


Figure 10



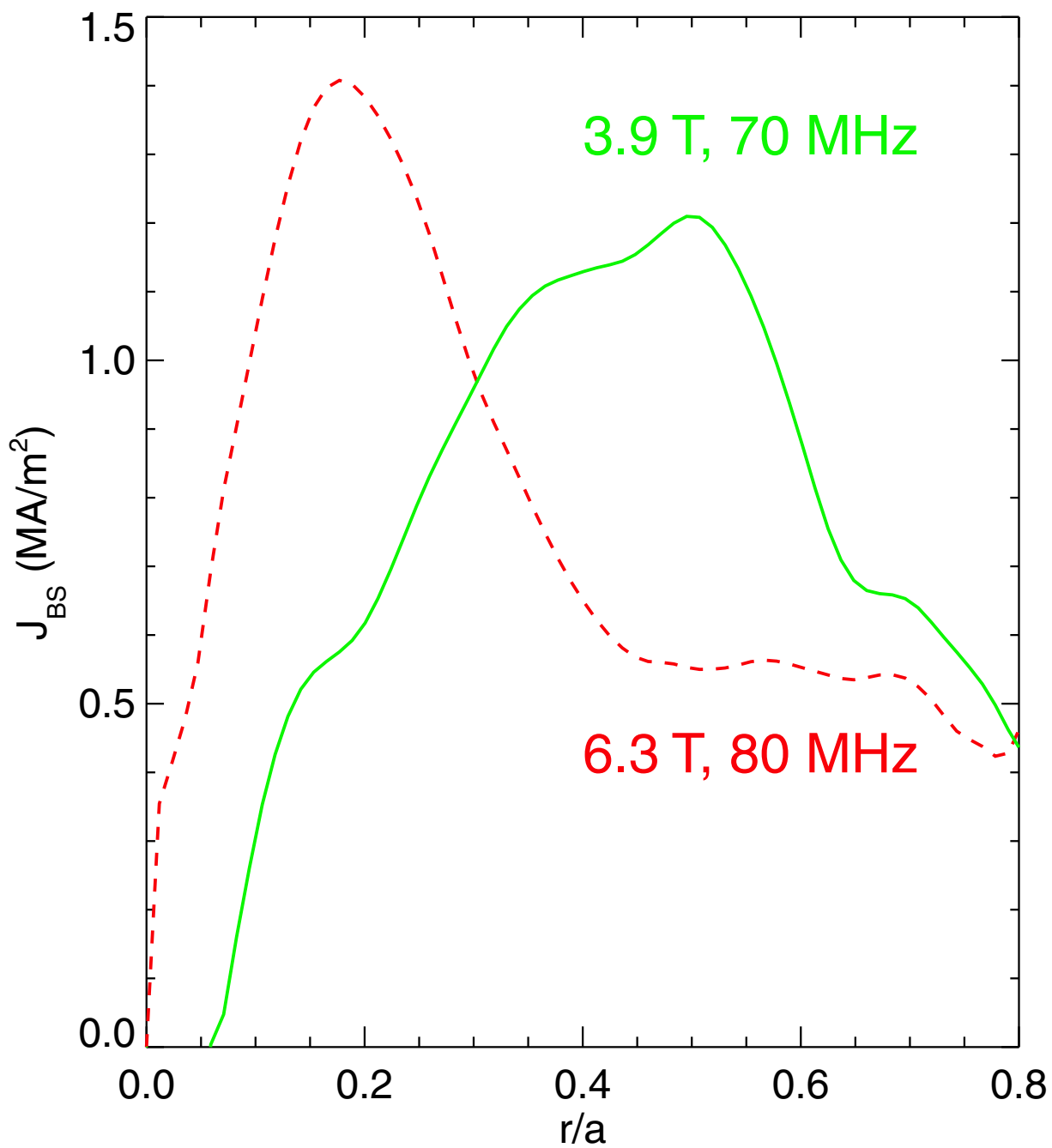


Figure 12